Inorganica Chimica Acta, 148 (1988) 123–131

Surface Coordination Chemistry of Noble-metal Electrocatalysts: Oxidative Addition and Reductive Elimination of Iodide at Iridium, Platinum and Gold in Aqueous Solutions

JOSE F. RODRIGUEZ, JOHN E. HARRIS, MICHAEL E. BOTHWELL, THOMAS MEBRAHTU and MANUEL P. SORIAGA*

Department of Chemistry, Texas A&M University, College Station, Tex. 77843, U.S.A.

(Received December 10, 1987)

Abstract

The oxidative addition and reductive elimination of the iodo ligand has been compared at smooth polycrystalline gold, platinum and iridium surfaces in aqueous solutions. On these three metals, the iodo species undergoes spontaneous oxidative chemisorption to form a close-packed monolayer of zero-valent iodine, the saturation coverage of which is limited by the van der Waals radius of the iodine atom; this oxidative addition process is further manifested by evolution of hydrogen gas from proton reduction. Elimination of iodine from these surfaces can be achieved by its reduction back to the anion either by application of sufficiently negative potentials or by exposure to ample amounts of hydrogen gas. On Pt and Ir, the reductive desorption of iodine is coupled with reductive chemisorption of hydrogen; consequently, the reaction is a two-electron, pH-dependent process. A plot of $E_{1/2}$, the potential at which the iodine coverage is decreased to half its maximum value, against pH yields information concerning the redox potential of the $I_{(ads)}/I^-_{(ads)}$ couple in the surface-coordinated state. On Au, where dissociative chemisorption of hydrogen does not occur, the iodine-stripping process is a pH-independent, one-electron reaction. The difference in the redox potentials $[E^\circ_{I(ads)} - E^\circ_{I(aq)}]$ for the $I_{(ads)}/I^-_{(ads)}$ and $I_{2(aq)}/I^-_{(aq)}$ redox couples was found to be -0.90 V on Au, -0.76 V on Pt, and -0.72 V on Ir. These values imply that the ratio of the formation constants for surface coordination of the iodine and iodide species ($K_{f,I}/K_{f,I^-}$) is 2×10^{28} on Au, 1×10^{26} on Pt, and 2×10^{25} on Ir.

Introduction

A review of the copious literature in surface science in the light of traditional concepts of coordination chemistry suggests that the interaction of inorganic and organic compounds with transition metal surfaces has several commonalities with the bonding of such ligands with metal centers in homogeneous or metal-cluster complexes [1]. The analogies are most striking under conditions, such as in aqueous electrochemistry, where the metal surface is initially covered by weakly-coordinating electrolyte or solvent molecules which are readily displaced by strongly-coordinating reagents [2]. We have recently initiated studies of the interaction of surface-active and reversibly electroactive moieties with noble-metal electrocatalysts. Our interest in these systems is based on the fact that chemisorption-induced changes in the redox properties of these compounds yield important information concerning the coordination/organometallic chemistry of the electrode surface. For example, the alteration in the redox potential of a reversibly electroactive species is a measure of the surface-coordination formation constant of the oxidized state relative to the reduced form; such behavior is dependent upon the electrode material. The case of the surface coordination of the iodo ligand at noble-metal electrodes provides an interesting study since this material is strongly surface-active and the properties of the iodine/iodide redox couple in the solvated state are well-known. Profound changes in the redox chemistry of the iodine/iodide couple brought about by the surface-coordination process are expected.

The chemisorption of iodide/iodine onto polycrystalline and single crystal Pt electrodes has been studied [3]; it has now been established that aqueous iodide or gaseous hydrogen iodide undergoes oxidative chemisorption to form a close-packed layer of zero-valent iodine accompanied by evolution of hydrogen gas. We recently studied the desorption of this zero-valent iodine from smooth polycrystalline Pt electrodes in protic [4] and aprotic [5] solvents. The two major findings are: (i) the redox potential for the $I_{(ads)}/I^-_{(ads)}$ couple in the chemisorbed state is nearly 800 mV negative of that for the unadsorbed couple; and (ii) the cathodic stripping of iodine from

*Author to whom correspondence should be addressed.

0020-1693/88/$3.50

Pt in aqueous media is always coupled with hydrogen chemisorption. In the present study, we examine and compare the oxidative addition and reductive elimination of the iodo ligand at polycrystalline Au, Pt, and Ir surfaces in aqueous electrolyte; variations in the surface-coordination chemistry of this ligand are anticipated because the subject electrodes have different propensities towards dissociative chemisorption of hydrogen, and are also likely to show different reactivities towards the iodo species.

Experimental

Smooth polycrystalline iridium, platinum and gold thin-layer electrodes were utilized in the present study. Thin-layer cells are suitable for surface electrochemical studies due to (i) the absence of diffusional mass transport to and from the cell which, combined with (ii) extremely small cell volumes helps to minimize surface contamination and (iii) enables isolation (for subsequent characterization) of species generated from surface reactions, and (iv) large area-to-volume ratios which ensure magnification of surface processes relative to those in solution. The fabrication of the thin-layer electrochemical cells [6] and the preparation of the smooth polycrystalline electrodes [7–9] were as described in the literature.

In between experimental trials, the electrodes were cleaned by sequential electrochemical oxidation (at $\geqslant$1.2 V) and reduction (at $\leqslant -0.2$) in 1 M H_2SO_4 [7–9]; surface cleanliness was verified by cyclic voltammetry in the same molar sulfuric acid solution. All potentials are referenced against the Ag/AgCl (1 M Cl^-) electrode. Experiments were carried out in 1 M H_2SO_4 (taken as pH 0), 1 M $NaClO_4$ buffered at pH 7 with $NaOH/NaH_2PO_4$ [10], 1 M $NaClO_4$ buffered at pH 10 with $Na_2CO_3/NaHCO_3$ [10], and in 1 M NaOH (taken as pH 14); the aqueous solutions were prepared using pyrolytically triply-distilled water [11].

Coordination of the iodo ligand onto the Ir, Pt and Au surfaces was accomplished simply by exposing the clean electrode with 1 mM NaI for 180 seconds at the same pH at which the reductive elimination experiments were to be performed. Excess (unadsorbed) iodide was removed by rinsing the thin-layer cell with pure supporting electrolyte; such rinsing does not remove the surface-coordinated iodine. The absolute surface coverage of iodine was determined by thin-layer coulometry in 1 M H_2SO_4 (regardless of the pH at which the iodine pretreatment was carried out) using two reactions attributable to the surface iodine:

(i) Anodic oxidation of chemisorbed iodine. This method is based on the fact that the total quantity of chemisorbed iodine is directly proportional to the

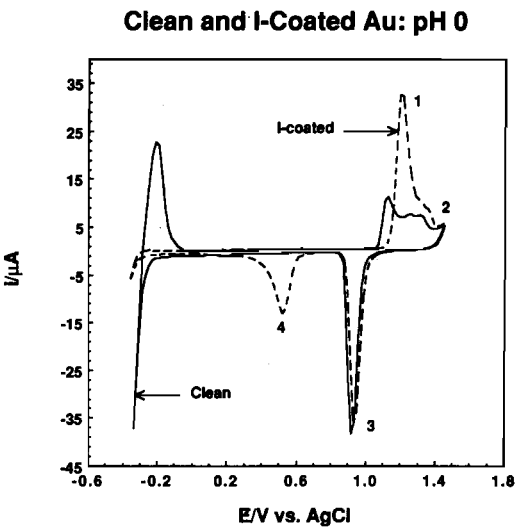

Fig. 1. Thin-layer cyclic current–potential curves for clean (solid curve) and iodine-pretreated (dashed curve) smooth polycrystalline gold in 1 M H_2SO_4. The peak numbers are as discussed in the text. Volume of thin-layer cell, V = 3.06 μl; electrode surface area, A = 1.07 cm^2; sweep rare = 3 mV/s; T = 298 K.

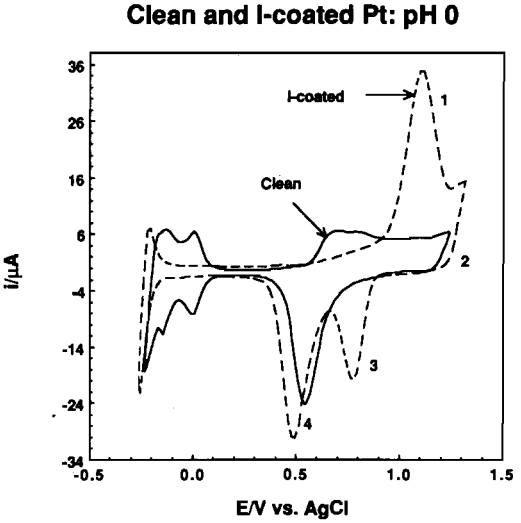

Fig. 2. Thin-layer cyclic current–potential curves for clean (solid curve) and iodine-pretreated (dashed curve) smooth polycrystalline platinum in 1 M H_2SO_4. The peak numbers are as discussed in the text. Volume of thin-layer cell, V = 3.86 μl; electrode surface area, A = 1.04 cm^2; sweep rate = 3 mV/s; T = 298 K.

measured charge for anodic oxidation of adsorbed iodine to aqueous IO_3^- [*cf.* peak 1 in Figs. 1 (Au) and 2 (Pt), peak 3 in Fig. 3 (Ir)]

$$I_{(ads)} + 3H_2O \longrightarrow IO_{3(aq)}^- + 6H^+ + 5e^- \quad (1)$$

The absolute coverage of the surface-coordinated iodine Γ_I (mol cm^{-2}) is given by

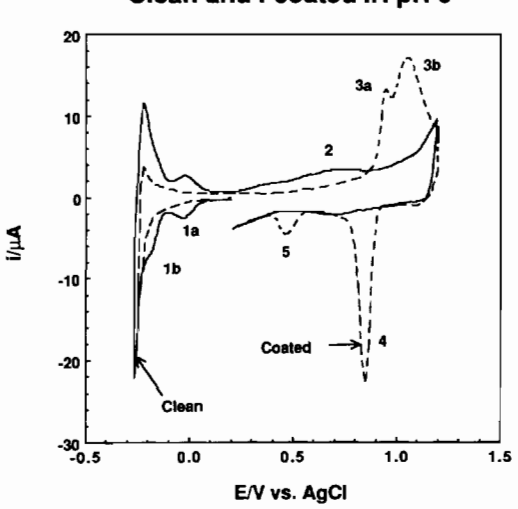

Fig. 3. Thin-layer cyclic current–potential curves for clean (solid curve) and iodine-pretreated (dashed curve) polycrystalline iridium in 1 M H_2SO_4. The peak numbers are as discussed in the text. Volume of thin-layer cell, $V = 3.74\ \mu L$; electrode surface area, $A = 1.40\ cm^2$; sweep rate = 2 mV/s; $T = 298$ K.

$$\Gamma_I = (Q - Q_b)_{ox,I}/5FA \quad (2)$$

where Q is the total charge for oxidation of both iodine and metal surface, Q_b is the background charge for oxidation of the metal surface in the absence of chemisorbed iodine, F is the Faraday, and A is the surface area (1.04 cm^2 for Pt, 1.07 cm^2 for Au, and 1.40 cm^2 for Ir) determined by underpotential hydrogen deposition [7] or by iodine chemisorption [8]. The use of an n value of 5 in eqn. (1) implies that iodine is zero-valent in the chemisorbed state.

(ii) Iodate reduction. The amount of chemisorbed iodine is also directly proportional to the measured electrolytic charge for reduction of aqueous IO_3^- [obtained in method (i) above] to aqueous I_2

$$IO_{3(aq)}^- + 6H^+ + 5e^- \longrightarrow 1/2I_{2(aq)} + 3H_2O \quad (3)$$

From this reaction [*cf.* peak 4 in Figs. 1 (Au) and 3 (Ir), peak 3 in Fig. 2 (Pt)], the iodine coverage is given by

$$\Gamma_I = (Q - Q_b)_{red,IO_3^-}/5FA \quad (4)$$

where Q is the total reductive charge, and Q_b is the background charge obtained in the absence of chemisorbed iodine. This method is limited to thin-layer electrodes.

It will be emphasized that, in eqn. (3), the use of an n value of 5 is independent of the chemisorption valency of iodine; hence, if iodine is indeed zero-valent in the chemisorbed state, then the following equality must hold

$$|(Q - Q_b)_{red,IO_3^-}| = |(Q - Q_b)_{ox,I}| \quad (5)$$

Results

The strong surface coordination of iodine at gold, platinum and iridium surfaces is established by the data presented in Figs. 1 to 3. These figures show current-potential curves for clean and iodine-pretreated Au (Fig. 1), Pt (Fig. 2) and Ir (Fig. 3) electrodes in 1 M H_2SO_4; the curves for the I-coated surfaces were obtained in the absence of bulk (unadsorbed) iodine/iodide species. For the clean electrodes, the general features of the voltammetric curves are as follows. (i) The reversible peaks observed at negative potentials are due to the reversible proton/hydrogen redox reaction. On Au (Fig. 1), only the hydrogen evolution reaction ($2H^+_{(aq)} + 2e^- \leftrightarrow H_{2(g)}$) is observed since dissociative chemisorption does not occur on this material. On Pt (Fig. 2) and Ir (Fig. 3), underpotential deposition peaks ($H^+_{(aq)} + e^- \leftrightarrow H_{(ads)}$) are observed prior to the hydrogen evolution reaction, reflecting the propensity of these metals to chemisorb hydrogen dissociatively; the hydrogen chemisorption peaks are dependent upon the crystallographic orientation of the electrode surface [9, 12, 13] and in some instances may be used to measure the active surface area of the platinum-group metals [7]. (ii) The irreversible peaks found at the more positive potentials are due to oxidation of the metal surface. The nature of these surface oxides depends upon the potential and pH of the solution; the thickness of the oxide layer, for example, increases as the potential is made more positive [9]. At more positive potentials, evolution of oxygen gas from electrolysis of the solvent occurs. On Au and Pt, the metal oxide surface may be reduced back to the metal at about 0.7 V; surface oxide reduction on Ir, however, cannot be achieved unless potentials close to the hydrogen evolution reaction are applied [9]. The morphology of the current–potential curves, especially in the hydrogen and oxygen regions, is critical in evaluating surface cleanliness [7].

When a clean Au, Pt or Ir electrode is exposed to aqueous iodide, a rapid negative shift of the 'rest' or equilibrium potential towards the hydrogen evolution region is always observed; this negative potential shift signifies the occurrence of an oxidative chemisorption process [2]. The general features of the voltammetric curves for the iodine-coated electrodes in 1 M H_2SO_4 are as follows. (i) The presence of surface iodine completely blocks hydrogen chemisorption on Pt (Fig. 2) and Ir (Fig. 3), and retards the hydrogen evolution reaction, most notably on Au (Fig. 1). (ii) The oxidation of the metal surface is also retarded by chemisorbed iodine; retardation is least on Au for which clean-surface oxidation is itself delayed relative to Ir and Pt. (iii) No iodine/iodide redox peaks are observed at about 0.4 V, the region where the bulk (unadsorbed) $2I^-_{(aq)} + 2e^- \leftrightarrow I_{2(aq)}$ reaction occurs;

this result arises because coordination alters the redox potential of the iodine/iodide couple in the surface-bound state. (iii) A large anodic peak [peak 3 in Fig. 1 (Au) and 2 (Pt), peak 4 in Fig. 3 (Ir)] is observed at $E > 1.1$ V; the charge under this peak is due to the anodic oxidation of chemisorbed iodine to aqueous iodate accompanied by oxidation of the metal surface itself [*cf.* eqns. (1) and (2)]. (iv) Reversal of the potential scan following anodic oxidation yields a cathodic peak [peak 4 in Figs. 1 (Au) and 3 (Ir), peak 3 in Fig. 2 (Pt)] attributable to reduction of the aqueous iodate to aqueous iodine [*cf.* eqns. (3) and (4)]. It is interesting to note that the iodate reduction peaks at Ir and Pt appear before surface-oxide reduction, while that at Au emerges only after oxide reduction. Peak 5 in Fig. 3 (Ir) is due to reduction of aqueous iodine to aqueous iodide; this occurs on Ir but not on the other two electrodes because, at these potentials, the Ir surface is still covered with hydrous oxides which block iodine chemisorption.

Figures 4 to 6 show thin-layer voltammetric curves for clean and iodine-pretreated Au at pH 7 (Fig. 4), Ir at pH 10 (Fig. 5), and Pt at pH 14 (Fig. 6); as before, experiments with the I-coated surfaces were performed in the absence of unadsorbed (bulk) iodide/iodine species. Important features to be noted in these three Figures are as follows. (i) On Au, two reversible peaks are observed on the iodine-coated surface which do not appear on the clean electrode; the potentials at which these peaks appear are independent of pH as was noted by experiments at pH 10. The peaks are clearly associated with the surface-coordinated iodine; since the rest potential for the

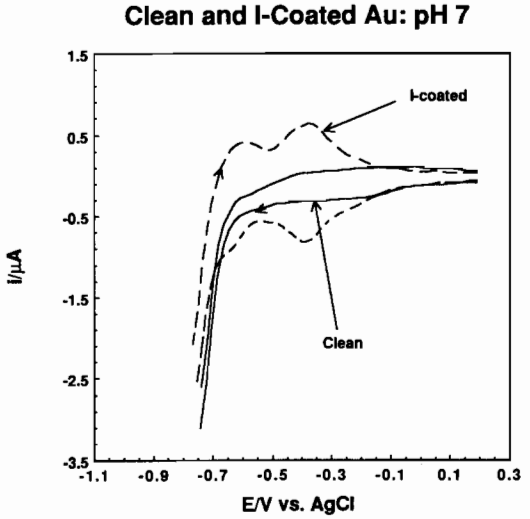

Fig. 4. Thin-layer cyclic voltammetric curves in the hydrogen region for a clean (solid curve) and iodine-pretreated (dotted curve) gold electrode in 1 M $NaClO_4$ phosphate-buffered at pH 7. Experimental conditions were as in Fig. 1.

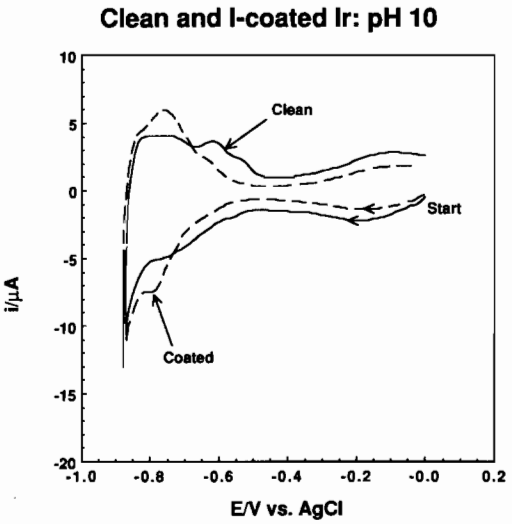

Fig. 5. Thin-layer cyclic voltammetric curves in the hydrogen region for a clean (solid curve) and iodine-pretreated (dotted curve) iridium electrode in 1 M $NaClO_4$ carbonate-buffered at pH 10. Experimental conditions were as in Fig. 3.

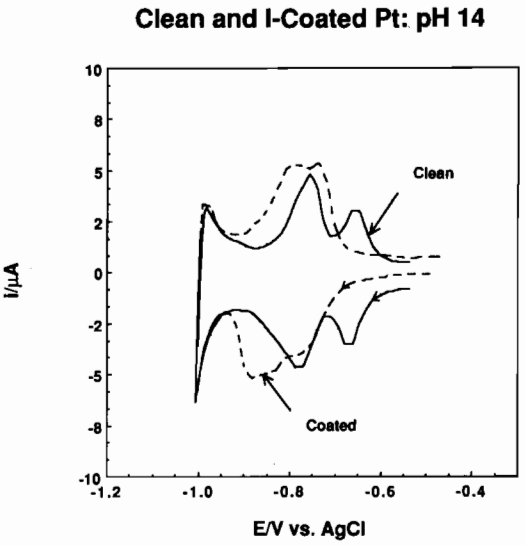

Fig. 6. Thin-layer cyclic voltammetric curves in the hydrogen region for a clean (solid curve) and iodine-pretreated (dotted curve) platinum electrode in 1 M NaOH (taken as pH 14). Experimental conditions were as in Fig. 2.

I-coated surface at pH 7 was about 0.3 V, the cathodic peaks are attributable to the (coverage-dependent) reduction of the chemisorbed iodine. (ii) A reversible redox peak is also noted on I-coated Ir which is not observed on the clean surface; likewise, this peak is attributable to the redox of chemisorbed iodine. (iii) Reversible redox peaks are also noted on I-coated Pt; these peaks are pH-dependent, as established by experiments at pH 10, and have been demonstrated to arise from the reductive

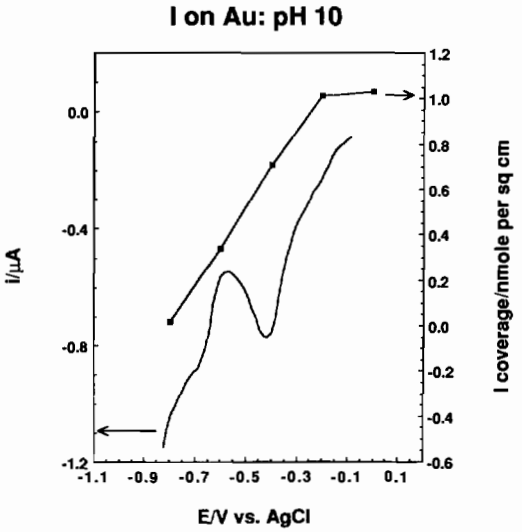

Fig. 7. Superimposed plots of the cathodic current (left ordinate) and absolute iodine surface coverage (right ordinate) in the hydrogen region for an iodine-pretreated gold electrode in 1 M $NaClO_4$ buffered at pH 10. Experimental conditions were as in Fig. 1.

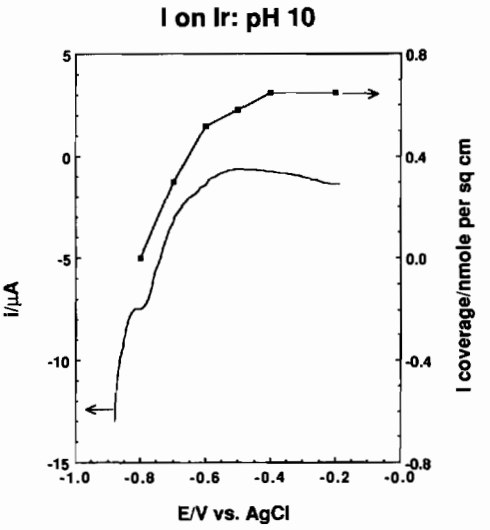

Fig. 9. Superimposed plots of the cathodic current (left ordinate) and absolute iodine surface coverage (right ordinate) in the hydrogen region for an iodine-pretreated iridium electrode in 1 M $NaClO_4$ buffered at pH 10. Experimental conditions were as in Fig. 3.

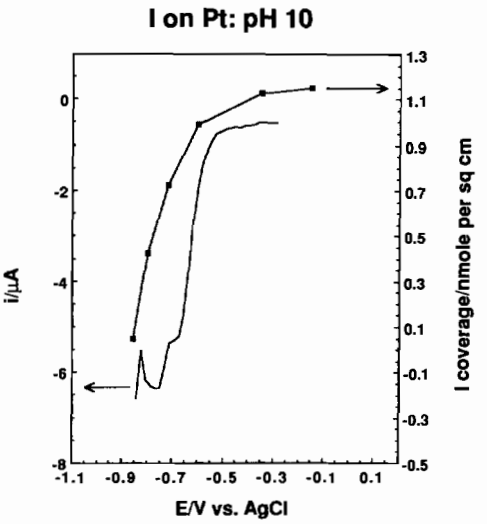

Fig. 8. Superimposed plots of the cathodic current (left ordinate) and absolute iodine surface coverage (right ordinate) in the hydrogen region for an iodine-pretreated platinum electrode in 1 M $NaClO_4$ buffered at pH 10. Experimental conditions were as in Fig. 2.

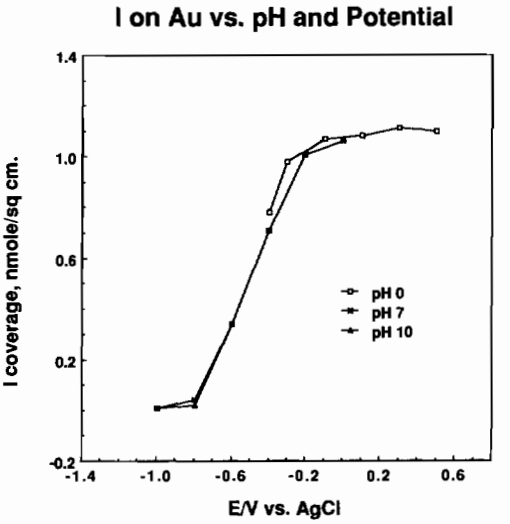

Fig. 10. Absolute surface packing density of iodine on polycrystalline gold as a function of potential in 1 M H_2SO_4 (taken as pH 0), 1 M $NaClO_4$ buffered at pH 7, and 1 M $NaClO_4$ buffered at pH 10. The solid lines interconnect the data points and do not represent any theoretical fit. Experimental conditions were as in Fig. 1.

desorption of iodine coupled with the reductive chemisorption of hydrogen [4].

Figures 7 to 9 provide evidence that the cathodic peaks exhibited by the pretreated surfaces are due to reductive elimination or desorption of surface-coordinated iodine. In these figures, cathodic current (left ordinate) and iodine surface coverage (right ordinate) are plotted simultaneously as functions of the applied electrode potential at Au (Fig. 7), Pt (Fig. 8) and Ir (Fig. 9). The decrease in iodine packing density is clearly correlated with the emergence of the reduction peak.

Plots of the absolute packing density of iodine Γ_I as functions of applied potential and pH are given in Figs. 10 to 12. It will be pointed out that Γ_I values at pH 0 could not be obtained at potentials more

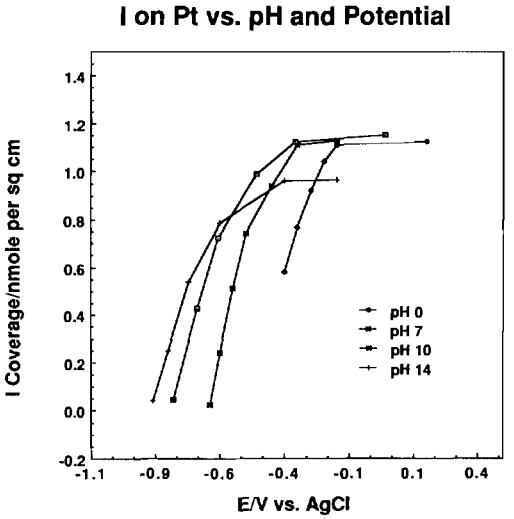

Fig. 11. Absolute surface packing density of iodine on polycrystalline platinum as a function of potential in 1 M H_2SO_4 (taken as pH 0), 1 M $NaClO_4$ buffered at pH 7, 1 M $NaClO_4$ buffered at pH 10, and 1 M NaOH (taken as pH 14). The solid lines interconnect the data points and do not represent any theoretical fit. Experimental conditions were as in Fig. 1.

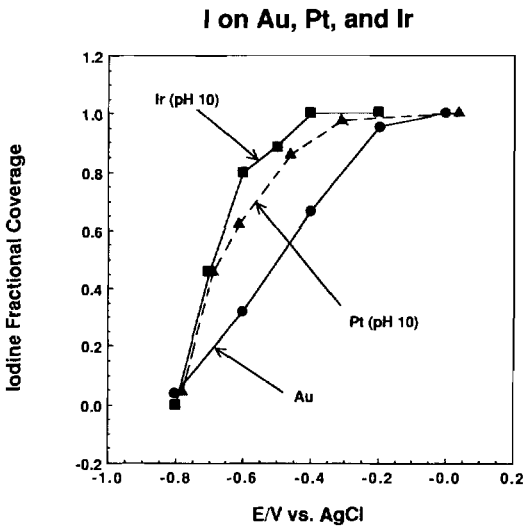

Fig. 13. Fractional surface coverage of iodine on polycrystalline gold (closed circles), platinum (closed triangles), and iridium (closed rectangles) as a function of potential in 1 M $NaClO_4$ buffered at pH 10. The solid lines interconnect the data points and do not represent any theoretical fit. Experimental conditions were as in Figs. 10 to 12.

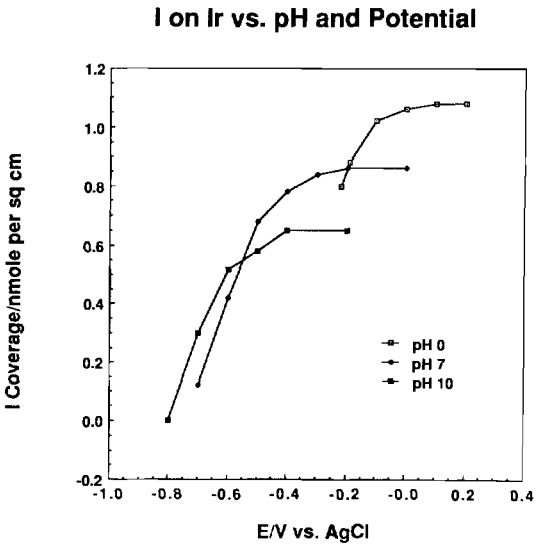

Fig. 12. Absolute surface packing density of iodine on polycrystalline iridium as a function of potential in 1 M H_2SO_4 (taken as pH 0), 1 M $NaClO_4$ buffered at pH 7, and 1 M $NaClO_4$ buffered at pH 10. The solid lines interconnect the data points and do not represent any theoretical fit. Experimental conditions were as in Fig. 1.

negative than shown in these figures because of extensive hydrogen gas evolution inside the thin-layer cell. The Γ_I *versus* E curves for Pt and Ir exhibit pronounced pH-dependence, whereas the Γ_I *versus* E plot for Au is unaffected by solution pH; these results are of course not unexpected in view of the above-mentioned findings that the redox peaks in Figs. 4 to 6 are pH-dependent at pretreated Pt and Ir but not at I-coated Au. It is interesting to note that the maximum iodine coverage at Ir is also pH-dependent. The latter observation is most probably due to the tendency of the Ir surface to form and retain surface hydrous-oxides [9]; that is, competitive surface coordination of the hydroxo ligand at pH $\geqslant$ 7 lowers the surface coverage of iodine.

The relative ease by which complete reductive elimination of iodine occurs at the three subject electrode surfaces can be appraised from the data in Fig. 13. This figure displays a plot of the fractional coverage of iodine θ_I (defined as $\Gamma_I/\Gamma_{I,max}$) at Au, Pt and Ir against electrode potential at a single pH, 10. It can be seen that complete desorption of iodine at Au takes place over a 600 mV region whereas removal of iodine at Ir and Pt is completed within a span of only 350 mV. Evidently, the propensity for Pt and Ir to chemisorb hydrogen facilitates the cathodic stripping of iodine from the electrode surface. In this context, it may be mentioned that the potential range at which desorption of iodine at Pt in anhydrous acetonitrile also occurs, is over a 600 mV region [5]; the impossibility of hydrogen electrosorption from aprotic media likewise retards complete removal of iodine.

The redox potential for the surface-coordinated iodine/iodide couple at Au can be determined directly from the redox peaks in Fig. 4 or the Γ_I *versus* E curves in Fig. 10. Similar direct measure-

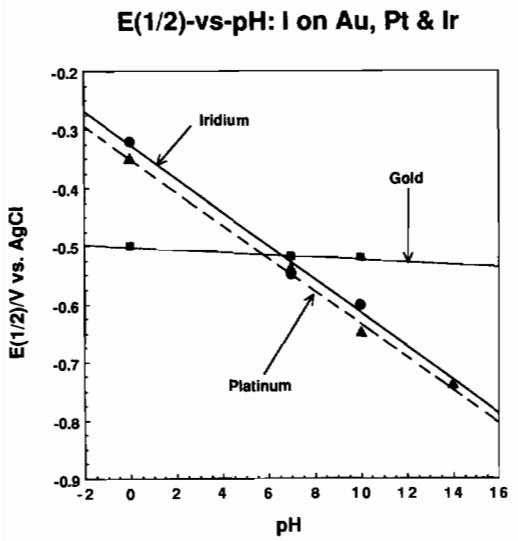

Fig. 14. Plot of $E_{1/2}$, the potential at which the surface coverage of iodine on gold (closed rectangles), platinum (closed triangles), or iridium (closed circles) electrodes is at half-maximum, against solution pH. The values in this plot were generated from the data in Figs. 10 to 12 as described in the text. The solid lines represent the linear least-squares fit (correlation coefficients ≥ 0.99).

ments at Ir and Pt are not possible because of the pH-dependence of the reductive elimination process at these surfaces. The pH-dependence may be factored out if the potential $E_{1/2}$ at which $\Gamma_I = 0.5\Gamma_{I,max}$ (where $\Gamma_{I,max}$ is the true maximum value obtained at pH 0) is plotted against pH. Based upon the data in Figs. 10 to 12, $E_{1/2}$ *versus* pH plots for Au, Pt and Ir are shown in Fig. 14; as discussed in detail in the next section, the intercept obtained by linear least-squares analysis of the data shown in Fig. 14 yields the pH-independent redox potential for the surface-coordinated iodine/iodide couple.

Discussion

Earlier work on the interaction of gaseous or aqueous hydrogen iodide with polycrystalline and single crystal Pt electrodes [3] have demonstrated that zero-valent iodine is the species which binds to the surface. The present results show that the same zero-valent species is also formed at polycrystalline Au and Ir. Oxidative chemisorption of the iodo ligand from aqueous media onto a gold surface, where dissociative adsorption of hydrogen is not a favorable process, probably occurs according to the following reaction

$$I^-_{(aq)} + H^+_{(aq)} \longrightarrow I_{(ads)} + 1/2H_{2(g)} \quad (6)$$

On Pt and Ir, where dissociative chemisorption of hydrogen is a facile reaction, the oxidative addition probably takes place as

$$I^-_{(aq)} + H^+_{(aq)} \longrightarrow I_{(ads)} + H_{(ads)} \longrightarrow I_{(ads)} + 1/2H_{2(g)} \quad (7)$$

The rapid shift of the rest potential towards the hydrogen evolution region which occurs upon exposure of these noble-metal surfaces to aqueous iodide attests to the formation of $H_{(ads)}$ and/or $H_{2(g)}$. Since the hydrogen gas produced remains inside the thin-layer cell, it can be reoxidized electrochemically to $H^+_{(aq)}$; the faradaic charge measured for such oxidation is consistent with the stoichiometry shown in eqns. (6) and (7) [2a].

Surface coordination of zero-valent iodine is also supported by the finding that the electrolytic charge for oxidation of chemisorbed iodine to aqueous iodate [509(12) μC/cm^2 at Au, 501(15) μC/cm^2 at Ir] is identical to that for reduction of aqueous iodate to aqueous iodine [505(12) μC/cm^2 at Au, 504(15) μC/cm^2 at Ir]; this means that the n value for the $I_{(ads)}$ to $IO_3^-{}_{(aq)}$ oxidation is 5, identical to that for the $IO_3^-{}_{(aq)}$ to $I_{2(aq)}$ reduction [*cf.* eqn. (5)]. The observation that removal of iodine from the surface requires application of reductive potentials (Figs. 7 to 9) further establishes the existence of zero-valent surface-bound iodine.

The inability of the gold electrode to dissociatively chemisorb hydrogen serves to simplify the reductive elimination of iodine from this surface; the reaction is a pH-independent, single-electron process

$$I_{(ads)} + e^- \longleftrightarrow I^-_{(ads)} \longleftrightarrow I^-_{(aq)} \quad (8)$$

for which the average (coverage-independent) redox potential $E^\circ_{I(ads)}$ may be taken as the intercept (−0.50 V) of the $E_{1/2}$ *versus* pH plot for the I-coated Au surface, Fig. 14. The validity of reaction (8), which is reversible as evidenced by the voltammetric curve in Fig. 4, may be tested from the data in Figs. 4 and 7 by application of Faraday's law of the form

$$(Q - Q_b)_{I,red} = nFA\Gamma_I \quad (9)$$

where $(Q - Q_b)_{I,red}$ is the electrolytic charge under the two (baseline-corrected) cathodic peaks for the I-pretreated Au electrode, n is the number of electrons involved in the reductive elimination of iodine, and Γ_I is the amount of iodine removed during the reduction process. Substituting the experimental data [$(Q - Q_b)_{I,red} = 100(10)$ μC; $\Gamma_I = 1.04$ nmol cm^{-2}; $A = 1.07$ cm^2] in eqn. (9) gives $n = 0.9 \pm 0.1$, consistent with reaction (8).

The reductive elimination of iodine at Pt and Ir surfaces, on the other hand, is a function of pH. Previous analysis of coulometric and voltammetric data indicated that the reductive desorption of iodine at Pt is pH-dependent because iodine removal is accompanied by hydrogen chemisorption according to [4]

$$I_{(ads)} + H^+_{(aq)} + 2e^- \longleftrightarrow H_{(ads)} + I^-_{(aq)} \quad (10)$$

Evidently, reaction (7) also occurs on polycrystalline Ir; its reversibility is manifested by the reversibility of the corresponding voltammetric curves in Figs. 5 and 6.

Although reaction (10) is complicated by proton reduction, it is possible to obtain an estimate of $E^{\circ}_{I(ads)}$, the pH-independent redox potential of the $I_{(ads)}/I^{-}_{(ads)}$ couple [reaction (8)] at Pt and Ir by adopting the following approach. The reversibility of reaction (10) allows the formulation of its Nernst equation as follows

$$E = K - 0.0296\,\mathrm{pH} \tag{11}$$

where the constant K is given by

$$K = E^{\circ}_{I(ads)} + E^{\circ}_{H(ads)} - 0.0296 \log[a_{I^{-}(aq)} a_{H(ads)}/a_{I(ads)}] \tag{12}$$

and a_i represents the activity of the ith species. $E^{\circ}_{H(ads)}$ is the standard potential for the reaction

$$H^{+}_{(aq)} + e^{-} \longleftrightarrow H_{(ads)} \tag{13}$$

Equation (11) states that, if $E_{1/2}$ is plotted against pH, a straight line with a slope of -0.0296 and an intercept of K will be obtained; such plots are given in Fig. 14. (It is important to mention that, in generating the data for Fig. 14 from Figs. 10 to 12, the following procedures were employed. (i) The $\Gamma_{I,max}$ value used to define $\Gamma_I/\Gamma_{I,max}$ was the true maximum value obtained at pH 0; as will be seen in the derivation of eqn. (15) below, this is required if the intercept K is to be interpreted correctly. (ii) The data points for pH 0 (1 M H_2SO_4) were obtained by a straight-line extrapolation of the last two or three measured values at the extreme negative potentials.) Linear least-squares analysis of the $E_{1/2}$ *versus* pH data for Pt and Ir yielded the following parameters: For Pt, slope = -0.028 and $K = -0.35$; for Ir, slope = -0.029 and $K = -0.33$. The slopes obtained are in excellent agreement with the predicted value of -0.0296 indicating that reaction (10) does indeed occur at these two surfaces.

At $E = E_{1/2}$, if determination of $E_{1/2}$ is based upon the true $\Gamma_{I,max}$ value at pH 0, half of the electrode surface is occupied by iodine and the other half is covered by hydrogen [3]. That is, $\theta_I = 0.5$ and $\theta_H \equiv \Gamma_H/\Gamma_{H,max} = 0.5$; the ratio $a_{H(ads)}/a_{I(ads)}$ thus becomes unity. Under these conditions, the intercept may be written as

$$K_{E_{1/2}} = E^{\circ}_{I(ads)} + E^{\circ}_{H(ads)} + 0.0296pI \tag{15}$$

where $pI = -\log a_{I^{-}(aq)} = -\log C_{I^{-}(aq)}$, $C_{I^{-}(aq)}$ being the solution concentration of the desorbed iodide. At $E_{1/2}$, the solution concentration of the desorbed iodide which remains inside the thin-layer cell is given by

$$C_{I^{-}(aq)} = 0.5\Gamma_{I,max}A/V \tag{16}$$

where V is the volume of the thin-layer cell (3.86 and 3.74 μl for the Pt and Ir thin-layer cells, respectively). $E^{\circ}_{H(ads)}$ is known to be dependent upon the crystallographic orientation of the electrode surface [9, 12, 13]. $E^{\circ}_{H(ads)}$ is therefore not a unique value for a polycrystalline surface. For the present purpose of estimating $E^{\circ}_{I(ads)}$, $E^{\circ}_{H(ads)}$ is simply taken as the potential at which $\theta_H \approx 0.5$; from Figs. 2 and 3, $E^{\circ}_{H(ads)}$ is seen to be approximately -0.1 V for both Pt and Ir. Substitution of the empirical data in eqn. (15) gives $E^{\circ}_{I(ads)} \approx -0.36$ V for Pt and ≈ -0.32 V for Ir. Since $E^{\circ}_{I(ads)}$ for Au is about -0.50 V, the trend in $E^{\circ}_{I(ads)}$ values is thus Au < Pt < Ir.

The $E^{\circ}_{I(ads)}$ values obtained here indicate that, upon surface coordination, the redox potential of the iodine/iodide couple is shifted in the negative direction by about 0.90 V on Au, 0.76 V on Pt, and 0.72 V on Ir. These chemisorption-induced redox potential shifts can be used to estimate the ratio of the formation constants for surface coordination of iodine and iodide

$$RT \ln[K_{f,I}/K_{f,I^{-}}] = -nF[E^{\circ}_{(ads)} - E^{\circ}_{(aq)}] - \Delta G^{\circ}_{d} \tag{16}$$

In eqn. (16), $K_{f,I}$ and $K_{f,I^{-}}$ are the respective formation constants for surface-coordinated iodine and iodide, $E^{\circ}_{(sol)}$ and $E^{\circ}_{(ads)}$ are the respective redox potentials for the $I_{2(aq)}/I^{-}_{(aq)}$ and $I_{(ads)}/I^{-}_{(ads)}$ couples, and ΔG°_{d} is the energy involved in the $I_{2(aq)} \rightarrow 2I_{(aq)}$ dissociation. Equation (16), which does not take into account coverage-dependence effects, is derived from the following thermodynamic cycle

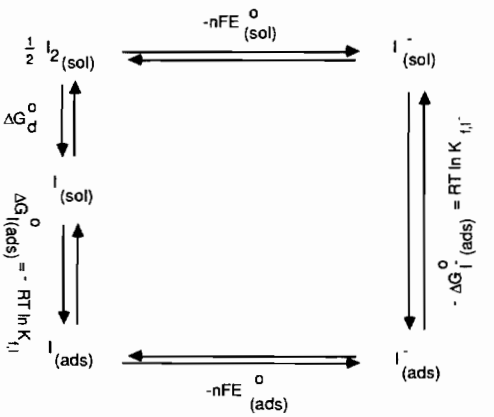

where $\Delta G^{\circ}_{I(ads)}$ and $\Delta G^{\circ}_{I^{-}(ads)}$ are the free energies of surface-coordination or iodine and iodide, respectively.

In calculating $K_{f,I}/K_{f,I^{-}}$ from eqn. (16), the following values have been employed: $E^{\circ}_{(ads)} - E^{\circ}_{(aq)} \approx -0.90$ V for Au, -0.76 V for Pt, -0.72 V for Ir, and $2\Delta G^{\circ}_{d} \approx$ the energy required to break the

I–I bond in the gas phase, 150 kJ/mol [14]. The calculated formation constant ratios are: 2×10^{28} on Au, 1×10^{26} on Pt, and 2×10^{25} on Ir. These exceedingly large values signify overwhelming preference by the subject metals for surface coordination of zero-valent iodine over iodide; comparison of the $K_{f,I}/K_{f,I^-}$ values indicate that this preferential surface coordination decreases as Au > Pt > Ir.

Acknowledgements

Acknowledgement is made to the Robert A. Welch Foundation and to the Regents of Texas A&M University for support of this research.

References

1 (a) M. R. Albert and J. T. Yates, Jr., 'A Surface Scientist's Guide to Organometallic Chemistry', American Chemical Society, Washington, D.C., 1987. (b) G. A. Somorjai, 'Chemistry in Two Dimensions: Surfaces', Cornell University Press, Ithaca, N.Y., 1981; (c) C. M. Friend and E. L. Muetterties, *J. Am. Chem. Soc., 103,* 767 (1981); (d) N. D. S. Canning and R. J. Madix, *J. Phys. Chem., 88,* 2437 (1984).

2 (a) M. P. Soriaga, E. Binamira-Soriaga, A. T. Hubbard, J. B. Benziger and K. W. P. Pang, *Inorg. Chem., 24,* 65 (1985); (b) M. P. Soriaga, J. H. White, V. K. F. Chia, D. Song, P. O. Arrhenius and A. T. Hubbard, *Inorg. Chem., 24,* 73 (1985); (c) B. C. Schardt, J. L. Stickney, D. A. Stern, D. G. Frank, J. Y. Katekaru, S. D. Rosasco, G. N. Salaita, M. P. Soriaga and A. T. Hubbard, *Inorg. Chem., 24,* 1419 (1985).

3 (a) R. F. Lane and A. T. Hubbard, *J. Phys. Chem., 79,* 808 (1975); (b) M. P. Soriaga and A. T. Hubbard, *J. Am. Chem. Soc., 104,* 2742 (1982); (c) J. L. Stickney, S. D. Rosasco, G. N. Salaita and A. T. Hubbard, *Langmuir., 1,* 89 (1985); (d) T. E. Felter and A. T. Hubbard, *J. Electroanal. Chem., 100,* 473 (1979); (e) G. A. Garwood and A. T. Hubbard, *Surface Sci., 92,* 617 (1980).

4 J. F. Rodriguez, T. Mebrahtu, B. G. Bravo and M. P. Soriaga, *Inorg. Chem., 26,* 2760 (1987).

5 B. G. Bravo, J. F. Rodriguez, T. Mebrahtu and M. P. Soriaga, *J. Phys. Chem., 91,* 5660 (1987).

6 A. T. Hubbard, *Crit. Rev. Anal. Chem., 3,* 201 (1973).

7 J. H. White, M. P. Soriaga and A. T. Hubbard, *J. Electroanal. Chem., 177,* 89 (1984).

8 J. F. Rodriguez, T. Mebrahtu and M. P. Soriaga, *J. Electroanal. Chem., 233,* 283 (1987).

9 (a) D. A. J. Rand and R. Woods, *Electroanal. Chem., 55,* 375 (1974); (b) M. W. Breiter, *Electroanal. Chem., 157,* 327 (1983); (c) S. Motoo and N. Furuya, *Electroanal. Chem., 167,* 309 (1984).

10 R. C. Weast, 'Handbook of Chemistry', CRC Press, Boca Raton, Fla., 1986.

11 B. E. Conway, H. Angerstein-Kozlowska, W. B. A. Sharp and E. E. Criddle, *Anal. Chem., 45,* 1331 (1973).

12 A. T. Hubbard, *Acc. Chem. Res., 13,* 177 (1980).

13 (a) A. T. Hubbard, *J. Vac. Sci. Technol., 17,* 49 (1980) 49; (b) P. N. Ross, in R. Vaneslow and R. Howe (eds.), 'Chemistry and Physics of Solid Surfaces, IV, Springer, New York, 1982; (c) A. S. Homa, E. Yeager and B. D. Cahan, *J. Electroanal. Chem., 150,* 181 (1983) 181.

14 F. A. Cotton and G. Wilkinson, 'Advanced Inorganic Chemistry', Wiley, New York, 1980.